## *Retrieval of vegetative fluid resistance terms for rigid stems using airborne lidar.*

Brasington, James; Richards, Keith S.; Antonarakis, A. S.; Muller, E.; Bithell, Mike

*Published in:*
Journal of Geophysical Research: Biogeosciences

*DOI:*
10.1029/2007JG000543

*Publication date:*
2008

*Citation for published version (APA):*
Brasington, J., Richards, K. S., Antonarakis, A. S., Muller, E., & Bithell, M. (2008). Retrieval of vegetative fluid resistance terms for rigid stems using airborne lidar. *Journal of Geophysical Research: Biogeosciences*, *113*(G2). https://doi.org/10.1029/2007JG000543

# Retrieval of vegetative fluid resistance terms for rigid stems using airborne lidar

A. S. Antonarakis,[1] K. S. Richards,[1] J. Brasington,[1] M. Bithell,[1] and E. Muller[2]

Received 5 July 2007; revised 30 October 2007; accepted 18 December 2007; published 30 April 2008.

[1] Hydraulic resistance of riparian forests is an unknown but important term in flood conveyance modeling. Lidar has proven to be a very important new data source to physically characterize floodplain vegetation. This research outlines a recent campaign that aims to retrieve vegetation fluid resistance terms from airborne laser scanning to parameterize trunk roughness. Information on crown characteristics and vegetation spacing can be extracted for individual trees to aid in the determining of trunk stem morphology. Airborne lidar data were used to explore the potential to characterize some of the prominent tree morphometric properties from natural and planted riparian poplar zones such as tree position, tree height, trunk location, and tree spacing. Allometric equations of tree characteristics extrapolated from ground measurements were used to infer below-canopy morphometric variables. Results are presented from six riparian-forested zones on the Garonne and Allier rivers in southern and central France. The tree detection and crown segmentation (TDCS) method identified individual trees with 85% accuracy, and the TreeVaW method detected trees with 83% accuracy. Tree heights were overall estimated at both river locations with an RMSE error of around 19% for both methods, but crown diameter at the six sites produced large deviations from ground-measured values of above 40% for both methods. Total height-derived trunk diameters using the TDCS method produced the closest roughness coefficient values to the ground-derived roughness coefficients. The stem roughness values produced from this method fell within guideline values.

**Citation:** Antonarakis, A. S., K. S. Richards, J. Brasington, M. Bithell, and E. Muller (2008), Retrieval of vegetative fluid resistance terms for rigid stems using airborne lidar, *J. Geophys. Res.*, *113*, G02S07, doi:10.1029/2007JG000543.

## 1. Introduction

[2] There is an increasing need to define the roughness of vegetation when modeling inundation flows on floodplains, and to do so at scales relevant to the simulation. This arises from the need to understand the flood risk implications of restoring woody vegetation to the immediate riparian zone and the floodplain. Better information on vegetation roughness of various types of vegetation is needed, including woody riparian species with different structural characteristics. Resistance equations need to take into account roughness in the form of below-canopy flow through the stems, as well as roughness for more complex tree morphology if and when flow enters the canopy. Roughness can then be parameterized in models at three different levels of dimensionality. This is first as a ''lumped'' roughness, such as for woody vegetation stems in one-dimensional and two-dimensional modeling; second, there is more localized spatially distributed roughness in two-dimensional modeling; and third, there may need to be a consideration of cell porosity and complex boundary implementation in the third (vertical) dimension. Thus the properties of vegetation need to be defined appropriately, dependent on modeling scale and dimensionality, and appropriate technology must be used to represent it in these various contexts.

[3] This paper outlines a strategy for extracting trunk roughness parameters from the appropriate remote sensing techniques. Until recently, light detection and ranging (lidar) techniques have focused on the interpolation and manipulation of point cloud data over large footprints to produce terrain models and simple vegetation roughness coefficients for usage in two dimensional flood simulations [*Mason et al.*, 2003; *Cobby et al.*, 2003; *Stoesser et al.*, 2003]. Trunk data to aid determination of the roughness of rigid stems are not recoverable directly from airborne lidar, but above-canopy information can be obtained, and allometric transfer functions derived from field measurements can then be used to infer trunk diameters and frontal areas. The above-canopy factors to be measured include the tree positions identified from the individual crown apices, total individual tree heights, and crown dimensions. The hydraulically relevant vegetation information required can be inferred from appropriate resistance equations.

[4] The necessity to evaluate flow resistance caused by vegetation in river environments has originally focused on the need to determine the roughness of vegetation lining channels. This has led to the assumptions that in-channel

[1]Department of Geography, Cambridge University, Cambridge, UK.
[2]Laboratoire Dynamique de la Biodiversité, CNRS, Toulouse, France.


0148-0227/08/2007JG000543$09.00

vegetation is stiff [e.g., *Pasche and Rouvé*, 1985], or flexible [e.g., *Kouwen et al.*, 1969; *Kouwen and Fathi-Maghadam*, 2000], or combinations of both [e.g., *Järvelä*, 2002]. It has been agreed that vegetation increases the flow resistance, changes the retention time of flooding, and alters deposition trends of sediments [*Yen*, 2002]. Yet, little has been done to attempt to further characterize vegetation especially when dealing with floodwater that comes in contact with floodplain vegetation, even if this is one of the most dominant sources of roughness in many river floodplains. An example of a successfully used set of resistance equations is presented in this paper, focusing on the parameterization of roughness of tree trunks.

[5] The aim of the present study was to estimate stem roughness coefficients in riparian forests with different structural characteristics, and in two river systems subject to different levels of river management. The first objective was to develop a tree detection and delineation algorithm to extract above-canopy forest information at the individual tree scale and to compare this to the method developed by *Kini and Popescu* [2004]. The second objective was to assess the accuracy of two lidar-derived techniques to recover individual tree heights, crown diameters, and trunk spacing and ultimately to derive stem diameters for different riparian forest patches. The accuracy of these variables was assessed by comparing the airborne lidar-derived terms with field measurements. The third objective was to determine stem roughness friction factors for below-canopy flow, and to assess the similarity of these terms to coefficients in guideline literature.

## 2. Study Areas

### 2.1. Site Descriptions

[6] Riparian forest data were obtained from two river systems in southern and central France. The first river reach investigated was on the River Garonne from downstream of Toulouse to upstream of its confluence with the River Tarn. The Garonne is a highly managed river, and there have been serious perturbations at the section investigated, and on the river in its entirety. The proximate floodplain is submerged approximately 30 d a year with flows of around 700 $m^3/s$ and a depth of about 2 m [*Décamps et al.*, 1988]. Centennial flood discharges can reach 6500 $m^3/s$ in this reach [*Muller et al.*, 2002].

[7] Stabilization of the bed and banks of the Garonne has diminished the duration that the floodplain is submerged, resulting in the disappearance of various biotypes. This reason, and also extensive farming on the floodplain has seen the rapid disappearance of riparian forests by 81% in the last two centuries. In the study reach, most of the woody vegetation on the floodplain was of planted poplar clones, consisting mainly of the hybrids of the European black poplar (*Populus nigra*) and the American cottonwood (*Populus deltoids*). There are a few lanes of regenerated natural riparian forest on the insides of meander beds, dominated by black poplar and containing some white willow (*Salix Alba*). Planted poplar forests in this section of the Garonne have a standard trunk spacing of around seven meters in each row of trees planted. Subsequently, each row is separated from the other by a similar average distance of seven meters. Natural riparian forests in this section are extremely dense due to the nonmigratory nature of the river channel. The spacing of individual trees or trunk clusters in these forested stands can be as small as 1.5–3 m both in the lateral and longitudinal directions.

[8] The second river reach investigated was of the River Allier directly upstream of Moulins in central France. Unlike the Garonne, the Allier is considered one of the few remaining natural (unmanaged) rivers in Western Europe. For this reason, the natural flora of the floodplain is very rich. The river is highly meandering at this section, and pioneer vegetation communities are common in spring and summer months due to the migratory nature of the river form and a continual renewal of sediments. The pioneer community consists of grasses, shrubs, and young softwood species, mainly of *Populus nigra* and *Salix alba*. It is estimated that 32% of the floodplain of the Allier around the Châtel-de-Neuvre area consists of pioneer vegetation, and around one third of the floodplain is occupied by trees or forests [*Peters et al.*, 2000]. Because of the dynamic and migratory nature of the Allier River, trees are not spatially constrained in growth and large swaths of sediment deposits can remain in winter. Here the densities of younger natural forests, which have seen their first couple of years of growth, are very dense with only a couple of meters separating each plant. Once these communities have experienced more floods, many individuals may be washed away, while the more robust trees remain. Therefore mature communities of natural poplar forest are sparsely populated with an average spacing of around four meters.

[9] The discharge regime of the Allier is highly variable due to the irregular precipitation upstream in the Massif Central. Proximate riparian vegetation is expected to be inundated every 1–2 years with a discharge of 800–1200 $m^3/s$, and every 5 years with a discharge of 1000 $m^3/s$ [*de Jong*, 2005]. The maximum discharge recorded at Moulins is 4700 $m^3/s$.

[10] In total, four forest sections were considered for the Garonne River sections and two for the Allier River section. These are three planted poplar types (young planted poplars [VY], intermediate planted poplars [VI], mature planted poplars [VM]) at the Verdun meander, and a natural forested section at the Monbequi meander [Mnb]. Two natural poplar forest types were considered for the Allier River, mature [ChM] and young [ChM] stands on the Châtel-de-Neuvre meander.

### 2.2. Data Collection

[11] Airborne lidar information and digital aerial photographs were obtained from flights organized by the Natural Environment Research Council Airborne Research and Survey Facility. The flights were scheduled to collect information on the reaches of the two rivers on 6 June 2006 for the Garonne and 8 June 2006 for the Allier. The 14 km section of the Garonne scanned was from UTM 31 coordinates [361500E 4851000N] to [353500E 4865000N], and the 20 km section of the Allier scanned was from coordinates [525000E 5128000N] to [526000E 5148000N]. This season was chosen in order that woody vegetation had leaves on them, and in order to have easier access to the sites. The airborne lidar data finally obtained had been georeferenced by the Unit for Landscape Modeling, Cambridge University. Details of the parameters and perfor-

**Table 1.** Performance Characteristics of the Airborne Lidar Data

| Parameter | Performance |
|---|---|
| System type | ALTM-3033 |
| Laser rep rate | 33333 Hz |
| Scan frequency | 21.7 Hz |
| Scan half angle | 20 |
| Average flying height, m | 1300 |
| Data recording | first and last pulse |
| Average point density, m | 1.9 |
| Laser processing software | Optech Realm v3.5 |
| Position accuracy | x, y < 1.0 m |
| Elevation accuracy WGS84 | z < 0.15 m |

mance of the data is shown in Table 1. The data obtained were in the form of point cloud coordinates (x, y, z) with intensity values.

[12] Two meanders were examined in detail on the River Garonne in June 2006, the first being near the village of Verdun-sur-Garonne (UTM31; 359500E 4854000N), and the second near the village of Monbequi (UTM31; 356000E 4861500N). The meander at Verdun is characterized as a site consisting almost entirely of commercially planted poplar clones of all ages. These poplars are heavily managed and pruned in order to produce tall, healthy, and commercially profitable trees. The ground in the summer consists of ploughed earth and dry, prone grasses distributed sparsely around the site. Three tree groups were chosen for investigation, all consisting of planted poplars of young, intermediate, and mature age groups. During data acquisition in June 2007, young planted poplars investigated were between 1 and 3 years old, intermediate poplars were 3–8 years old, and the mature poplars were of around 10–12 years old. The sites are around 100–300 m from the low-flow water's edge. In total, 196 trees were measured. The meander at Monbequi is characterized by very dense natural black poplars close to the river edge. The surface consists of gravely sediments with dense nettles in some areas during the summer months. At this site, 96 trees were measured.

[13] One meander section was examined on the River Allier in the month of February 2007 near the village of Châtel-de-Neuvre (UTM31; 525250E 5140350N). In this meander section most of the surface was bare, consisting of variously sized sediments, and the areas that were vegetated were sparsely distributed. The main species again was *Populus nigra* with several of its hybrids. A secondary species was *Salix alba*. Forty poplars were considered for measurement, and were between 0 and 100 m from the water edge. The natural trees measured were mature (20 trees) and young natural black poplar (20 trees). These 40 trees were selected so that they would be relatively near the riverbank, and to gain a representative sample of natural riparian trees in the area.

[14] Ground data were acquired for each individual tree in each location where possible. First, the trunk diameter of each tree was estimated at breast height (DBH), by measuring the circumference at breast height (1.3 m) with a meter tape, and calculating the diameter; the precision of this was millimetric. Each tree height was measured where possible with a LaserAce 300 instrument. This is a handheld reflectorless laser measurement system that can measure distances and heights of up to 300 m using an integrated digital inclinometer. The laser has a precision of 10 cm at intermediate distances (100–200 m), and the inclinometer has a precision of 0.3°. Crown dimensions were measured with a 30 m tape at ground level in four perpendicular directions using the trunk as the center. Finally, trunk spacing was measured. In order to have the quickest and most accurate representation of each tree position, central coordinates of trunks were extracted from Terrestrial Laser scans produced at the Garonne River in June 2006. At the Allier, handheld GPSs were used to obtain general positions of the trees measured.

## 3. Methods

### 3.1. Terrain Model

[15] Before it is possible to detect and delineate individual trees, a canopy height model needs to be created from which to estimate relative heights of objects from the ground, rather than absolute WGS84 elevations. Thus there is an initial need to develop a DTM of the areas investigated.

[16] One of the main issues in using airborne lidar to interpolate terrain models has always been that over densely forested areas most of the points returned have been intercepted by the canopies. Even last pulse points often do not make it to the ground, so producing a terrain model must depend on its eventual application or use. In the recent past, lidar has been used as a major source of elevation data for the purpose of producing a quality terrain model [*Lohr*, 1998; *Lloyd and Atkinson*, 2002], supplanting photogrammetrically derived DTM methods [*Adams and Chandler*, 2002; *Lane et al.*, 2003]. The application of lidar data to produce elevation models has involved the interpolation of raw point clouds into a rasterized DTM, using the last lidar wave return. This has been done with iterative filtering of the last pulse surface layer using various kernel sizes, as in the work by *Suárez et al.* [2005]. Iterative filtering techniques for the creation of terrain models though, cause the original minima point cloud coordinates to be lost at this early stage. There is an advantage in dealing with original point clouds to create terrain models rather than evening-out raster interpolations, as this does not skew the elevation values in this early stage of data manipulation. In other words, the terrain model could contain the actual low elevations points picked up by the lidar sensors. *Anderson et al.* [2006], for example, avoided filtering interpolated raw points by reducing the density of points in the original point cloud to 25% with an optimum resolution for the DTM of 10 m.

[17] Bare earth models were created for the Garonne and Allier meander floodplains described above. A method was developed to create a terrain model from the original airborne lidar point clouds aided by C++ programming. This algorithm is divided into five steps: determining the data set dimensions, development of containers, placement of raw points in containers, finding minima within each container, and finally removing outlying points.

[18] First, the edge coordinates are established in order to define the geographical extent of the data. This involves obtaining minima and maxima easting and northing values for the data set. These edge coordinates are then used as vertices to create cells over the defined data set. The cells act as a uniform grid, cutting the point cloud with a user-

defined resolution in meters. Each grid cell is assigned the points that fall within its borders, and a search is performed for the point with the lowest elevation, and this is then output with its original $x$, $y$, and $z$ coordinate. Once all the grid cells have been searched, all the minimum coordinates for the specified resolution are output into a text file. Grid cells that contain no points return minima elevation $xyz$ coordinates of [−999 0 10000]. This new minimum point cloud was then used to interpolate a terrain model using a triangular irregular network (TIN). However, the resulting triangulation usually contained jagged and extreme elevation points, especially in dense forested sections. Thus these outlying extreme points were identifying and deleted.

[19] A TIN was created from the minima points, containing information on each individual triangle vertex, as well as the three vertices of each triangle. Each individual irregular triangle was the conjunction of three nearest neighbors. An iterative code was written in Matlab to read the triangle identifiers and the vertex coordinates of each triangle, to recognize the three elevation values for each triangle, to spot triangle faces that had elevation differences of more than the 5 m threshold, and to delete each point identified as an outlier. The output was an $xyz$ point cloud with the original coordinates of each identified minimum point. The threshold for omitting outlying elevation values was taken to be points that were more than 5 m above their nearest neighbor. This is because a lower threshold would mean deleting values on steep faces, and higher thresholds would result in outlying values being missed. A lower threshold of 3 m was attempted for the three meander sites resulting in around one fifth of the triangles interpolating floodplain edge cliffs to be deleted. An 8 m threshold was also attempted for the sites, resulting in many of the outlying points near the low flow river's edge not to be detected.

### 3.2. Canopy Height Model

[20] A canopy height model (CHM) was derived by taking the difference between the digital surface model (DSM) and the DTM. The DSM was also derived by binning the data into a regular grid of cells, and searching for maximum heights in each cell. This algorithm was used instead of a direct raster interpolation of the first pulse point cloud data, because raster interpolations average elevation values when using a grid resolution containing more than one point, and this tends to smooth out the extremes.

[21] The desired resolution of the CHM had to be small enough to be able to include points that would ultimately represent tree apices and crown edges. Thus the resolution had to be the same or smaller than the crown diameters of the youngest poplars measured, i.e., 1–2 m. The $x$ and $y$ resolution of a cell that was defined depended on the point density of each individual vegetated area investigated, and could be from 0.1 m to over 3 m in some places. Such a range of point spacing can be attributed to the movement of the plane during data acquisition and to data overlapping, as well as to zero reflectance from water surfaces. A good surface representation of the forested section had to be achieved, and vegetated areas with dense points were thus assigned maximum values every 0.5 m, while in areas with more sparse data, the resolution was 1 m. A TIN was then created for the maxima, and a raster interpolation was created with the desired resolution.

[22] Three canopy surface models were thus created from the regional maxima of the raw point cloud data. The first was for the Verdun meander, which incorporated the three planted poplar sites of different ages. The resolution of the interpolated raster was set to 1 m for simple manipulation, as the average point density of the point cloud was 1.3 m. The raster interpolation of the Châtel-de-Neuvre meander on the Allier was also simplified to a 1 m resolution, as the average spacing of raw points was between 1 and 2 m. The average spacing of the densely vegetated Monbequi meander site was around 0.7 m, so the raster interpolation of the points was set to have a grid resolution of 0.5 m. Subtracting the terrain model from the surface model subsequently created the CHMs with resulting resolution of 1 and 0.5 m depending on the sites. To achieve this, the terrain model is binned down to a 1 m resolution, but the detail of the canopies in the surface models remained at 1 or 0.5 m.

### 3.3. Resistance Calculations

[23] Roughness estimates for rigid stems need to be obtained using extractable vegetation parameters. The Darcy-Weisbach friction factor has been used extensively in ascertaining vegetation roughness. This theoretical friction factor for flow resistance caused by vegetation roughness can be defined [cf. *Järvelä*, 2004] as

$$f = 4C_d \frac{A_p}{A_b} \tag{1}$$

[24] In equation (1), the friction factor ($f$) is related to the drag coefficient ($C_d$), the projected area of the blockage ($A_p$), and the bottom area ($A_b$). *Lindner* [1982] sought to derive an empirical formula of the drag coefficient for simple vegetated stands, through experimental studies performed with cylindrical elements. This drag coefficient formula is

$$C_d = \left(1 + 1.9\frac{d}{a_y}C_{d\infty}\right)\left(0.2025\left(\frac{a_x}{d}\right)^{0.46}C_{d\infty}\right) + \left(\frac{2a_y}{a_y - d} - 2\right) \tag{2}$$

and is obtained from the diameter of an element or trunk ($d$), the longitudinal ($a_x$) and the lateral ($a_y$) distances between the elements, and $C_{d\infty}$ is the drag coefficient of a single cylinder in an ideal 2D flow. The two terms on the right hand side of the above equation represent blockage and free surface effects, respectively. The term $C_{d\infty}$ is reported to be of 1.0–1.2 for typical Reynolds numbers. The friction factor $f$ [*Lindner*, 1982] is

$$f = \frac{4dh}{a_x a_y}C_d \tag{3}$$

[25] Equation (3) has been used subsequently in several studies [*Pasche and Rouvé*, 1985; *Järvelä*, 2004; *Stoesser et al.*, 2003]. The depth of flow ($h$) is multiplied by the average diameter of the cylindrical trunks ($d$) to create a variable to represent the projected area ($A_p$). Friction factor $f$

was converted to Manning's $n$ using the following equation from *Fathi-Maghadam and Kouwen* [1997]:

$$n = \sqrt{f}\left(\sqrt{\frac{h^{1/3}}{8g}}\right) \tag{4}$$

[26] Characteristics of the vegetation such as the trunk area are not visible in airborne lidar data. Hence, transfer function relationships need to be established to relate known and detectable factors of the tree geometry to these unobservable factors. Since the required relationships are between parts of living objects, the rules of allometry were applied, allometry being the study of size and its biological consequence [*McMahon*, 1973]. The allometric relationships used in this study are power functions between two variables $Y$ and $X$ of the form $Y = Y_0X^{\alpha}$, where $Y_0$ is the allometric constant or proportionality factor, and $\alpha$ is the scaling exponent or biological variable. The variables are both independent, so the appropriate regression model, according to *Niklas* [2004], is the reduced major axis (RMA) regression.

[27] The relevant tree variables that can be measured from airborne remote sensing are the individual tree heights, the crown dimensions, and the locations of trees. Allometric power functions can be used to infer the trunk diameters from above-canopy characteristics, which are identified using individual canopy detection algorithms. In fact, there is growing demand for the identification of forest properties in a variety of fields, from hydraulic engineering to forest fire assessment and wildlife conservation. This involves scales from forest stands to individual trees in a stand. The identification of tree positions and their above-canopy characteristics from remotely sensed data can provide criteria by which to locate the tree trunk and define its diameter at breast height, and this can then form the basis for estimation of vegetation frontal area in resistance equations.

### 3.4. Tree Crown Identification Algorithms

[28] Various algorithms exist to identify two key factors from airborne remotely sensed data: the individual crown heights and widths, and the positions of the tree trunks. Before the possibility of acquiring lidar data, tree detection and delineation was performed with multispectral imagery, or digital aerial photographs. Research that sought to identify canopy height maxima and crown edges using high-resolution remotely sensed imagery include that by *Pouliot et al.* [2002] and *Culvenor* [2002]. Here, tree maxima were determined from a fixed search window, identifying the brightest pixels in a crown as the tree apex, and adjacent dark pixels as the edges of the crown.

[29] More recently, studies have used airborne lidar to identify forest characteristics as the peaks in a canopy height model, derived from the difference between a terrain (last pulse) model and a surface (first pulse) model. The identification of individual trees, and the estimation of their absolute heights has been a priority in remotely sensed forest detection methods [*McCombs et al.*, 2003; *Koukoulas and Blackburn*, 2005; *Andersen et al.*, 2001; *Popescu et al.*, 2003; *Brandtberg et al.*, 2003]. Studies have also used small footprint airborne lidar to determine the tops of individual trees and their crown diameters using ground-derived regression relationships between the total tree height and the crown spread [*Kini and Popescu*, 2004; *Tiede et al.*, 2005; *Pitkänen et al.*, 2003]. This creates a variable maxima search window depending on the height-crown allometric regressions. This approach has generally been applied to sparsely spaced trees, or on forest plantations of even spacing, with little application to dense forests such as those in riparian zones. Attempts have also been made to try and estimate tree information by extracting relevant factors from airborne lidar data such as tree stem volume [*Hyyppä et al.*, 2001; *Maltamo et al.*, 2006], leaf area index [*Roberts et al.*, 2005] and stand level biomass [*Popescu et al.*, 2003]. Descriptions of the two algorithms used in this study are described in the subsequent sections.

#### 3.4.1. Tree Detection and Crown Segmentation (TDCS)

[30] The tree detection and crown segmentation (TDCS) method is a combined set of algorithms for detecting individual tree maxima and crown diameters from a large-scale, lidar-derived canopy height model. The output information is in the form of coordinates of trees with their apices and their crown diameters. The method is described below, and also in the flowchart in Figure 1.

[31] The input into the algorithm is a canopy height model of the three meandering areas on the rivers Allier and Garonne. The TDCS algorithm was written as a MATLAB code with the help of the Image Processing Toolbox 5.4. The first element of the algorithm is the identification of trees and the extraction of their heights. The method was based on applying variable search windows to identified tree maxima. Various variable window techniques for identifying trees have been used [*Kini and Popescu*, 2004; *Tiede et al.*, 2005; *Pitkänen et al.*, 2003] and attempt recognition of a single apex per individual tree. These studies have also defined the need to recognize the relationship between the tree height and the crown width from ground measurements to define the sizes of the variable window.

[32] Canopy maxima were initially defined as the local maxima in $3 \times 3$ m windows above a height of 2 m from the canopy height surface previously created. This resolution and elevation was preferable to using the elevations for every interpolated meter pixel, as it avoids ground topography and it reduces computational time in the detection of trees. At this moment, some crowns contained multiple maxima for single crowns. Each tree in theory contains a different elevation related to a different crown spread. From ground measurements of poplars on the three meanders studied in France, allometric relationships were developed relating the crown widths of individual trees to their heights. Therefore each individual initial crown maximum previously identified was subsequently attributed an allometrically derived crown radius, and circles (representing a crown) of that radius were created around each maximum. Crown circles were next divided into groups depending on their respective sizes. Then iteratively, tree apices that fell in the 'shadow' of taller and larger trees were identified, and deleted. The shadow of a taller tree defines the circular crown area of a taller tree with a larger crown area. Therefore, shorter tree apices that fell in the same circular area as a larger tree were considered as being part of the

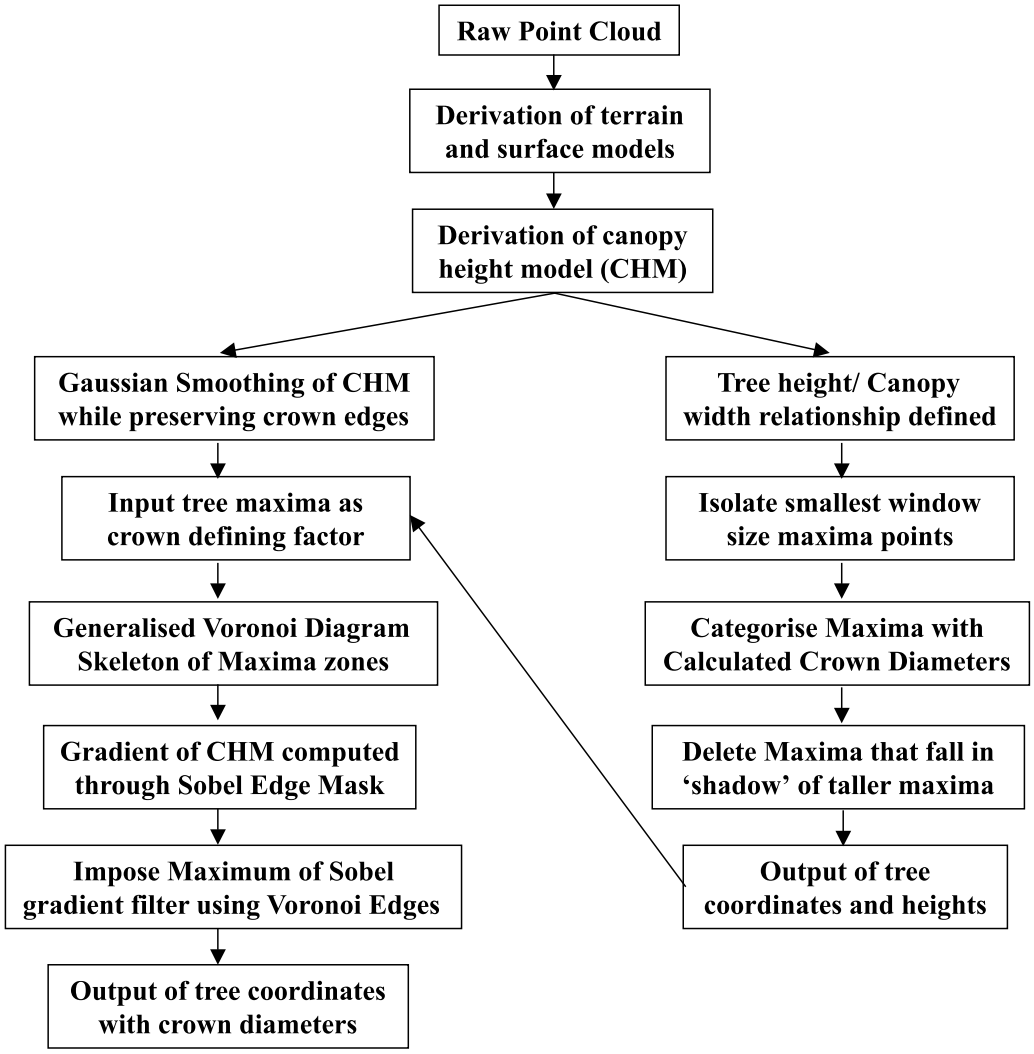


**Figure 1.** Flowchart of the TDCS algorithms using a lidar-derived canopy height model (CHM).

same canopy and deleted. The remaining maxima values were taken to be the tree identifiers and the tree apices.

[33] The second element of the algorithm was the Maxima Controlled Watershed Segmentation (MCWS) method based on *Soille* [1999] and from the Matlab image processing toolbox (MathWorks, Image Processing Toolbox 5.4, cited 24 February 2007, available at http://www.mathworks.com/products/image/demos.html). The inputs required for this component of the TDCS algorithm are the canopy height model and the tree maxima identified above. This function serves to delineate crowns from canopy height models using defined maxima to pinpoint each tree. The first step was the Gaussian smoothing of the CHM using one $x$ and $y$ dimensional smoothing iteration, which evens out the canopy undulations, but does not destroy the edge of the crowns. Edge preservation methods prior to crown delineations have also been used by *Brandtberg et al.* [2003], *Pitkänen et al.* [2003] and *Pouliot et al.* [2002] and serve to create individual crowns that have more uniform elevations without tampering with the crown edges. The canopy foreground of the raster layer is then fixed with the prior knowledge of the positions of individual trees. The background or edges of the crown subsequently need to be marked. This was done by computing the skeleton of influence zones (SKIZ), also-called generalized Voronoi polygons (MathWorks, 2007). This creates polygons around each crown identified with a maxima value, so that each treetop has an adjacent area circumscribing it. The gradient of the smoothed CHM is then needed to identify the points of inflection on the crown's edge, and is performed using a Sobel Edge filter that is again an edge-emphasizing filter [*Kanopoulos et al.*, 1988]. Consequently, this image is coupled with the Voronoi polygons. When the watershed algorithm is finally applied, the crown is identified from the lowest gradient in proximity to the crown, but does not pass the Voronoi polygon edge. The average diameter of each individual tree crown is calculated, and the final output is the coordinates of the trees with information on their heights and crown diameters.

#### 3.4.2. TreeVaW

[34] The tree variable window method is an integrated lidar processing software package (TreeVaW) capable of extracting forest inventory parameters at the level of individual trees from a lidar-derived canopy height model (CHM). This method, developed by *Popescu et al.* [2003] and *Kini and Popescu* [2004], focuses on algorithms that

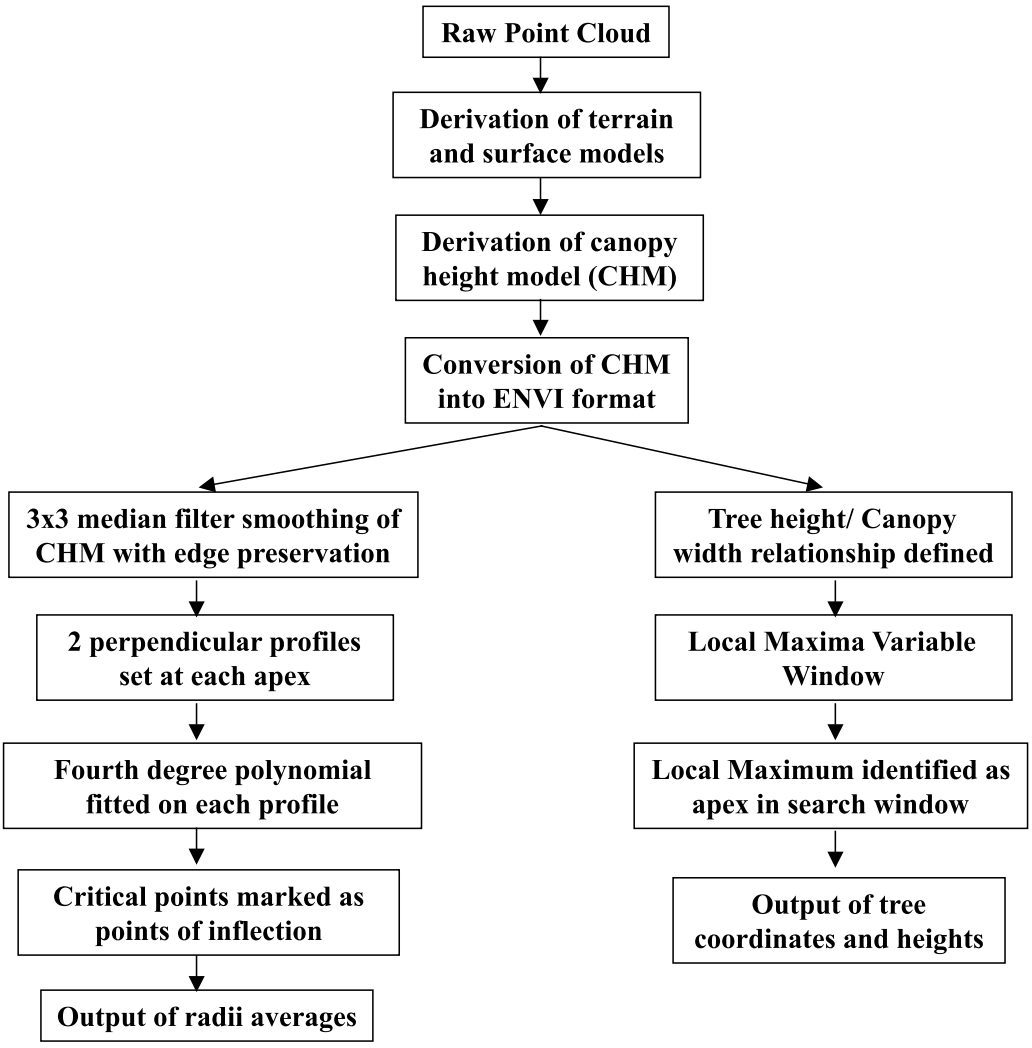


**Figure 2.** Flowchart of the TreeVaW algorithm using a lidar-derived canopy height model (CHM).

support (1) individual tree identification, (2) height measurements, and (3) crown width measurements. The input into TreeVaW is a lidar-derived, rasterized, canopy height model in an ENVI format (generalized raster data format) or can be from a spectral aerial image. ENVI stands for Environment for Visualizing Images and is an image processing system targeted at users of satellite and airborne remote sensing data. The output file ultimately gives the coordinates of the tree apices, their height, and their average crown width, and can be imported into GIS systems. The method is described below and also in the flowchart in Figure 2.

[35] To apply this method, the CHM derived in the previous sections is first converted to the ENVI standard format using the ENVI 4.2 program. This in essence changes the point data format, and attached an ENVI header to the rasterised file. Tree identification and height determination identifies tree apices through a user specified moving window. The variable window size is derived from the linear or quadratic relationship between tree heights and crown width, i.e., the higher the tree the larger the crown width. The equations are not allometric as described in a previous section. When using these equations, the algorithm reads the height value at each pixel and calculates the window size to search for the local maxima. If the current pixel corresponds to the local maxima within the desired window, then it is flagged as a treetop. In other words, local maxima are flagged if a maximum is found where its defined horizontal extent (linear relationship) does not define any point higher. Once the tops are established and the tree is identified, the heights are measured, as the elevation of the raster pixel.

[36] For crown width measurements, preprocessing is performed and involves applying a $3 \times 3$ median filter to the CHM in order to smooth the highly complex surface representing the top of the canopy. The median filter suppresses noise without affecting the CHM shape. Also, it is an edge preservation filter, so the crown delineation is preserved. The locations of the trees are then used to extract two perpendicular profiles of the CHM, centered at the treetops. A fourth degree polynomial is fitted on each profile. The second derivative of the profile polynomial is used to investigate the change in slope. The sign of the first derivative indicates whether the graph of the fitted function is rising or falling, and the sign of the second derivative indicates where the fitted function is concave (negative) or

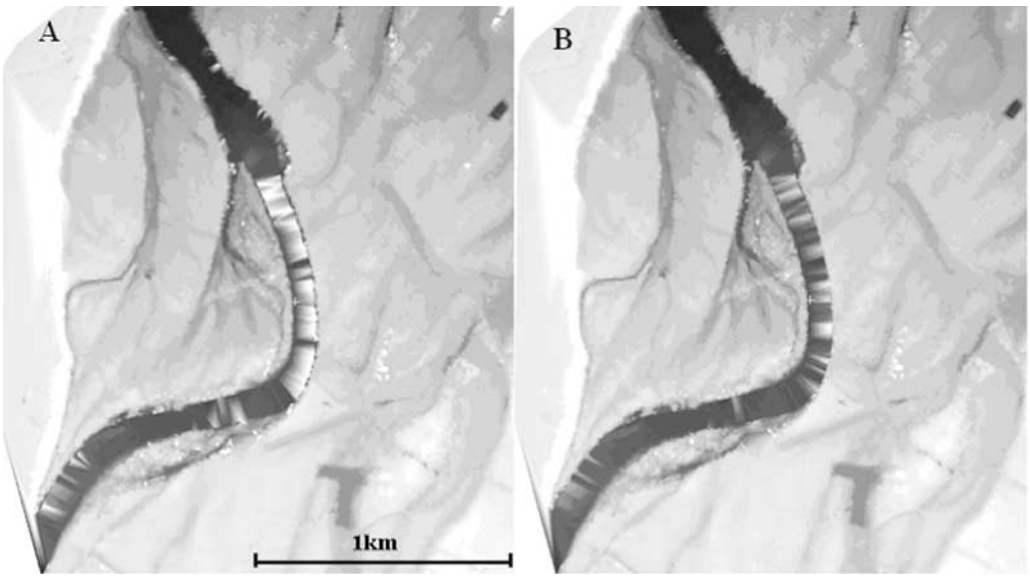


**Figure 3.** Terrain model at the Verdun meander on the Garonne River before (A) and after (B) the omission of outlying point elevations.

convex (positive). Points of inflection at the edge of the concave or convex function are marked as critical points (marking the crown edge). The Crown Width can finally be calculated as the difference between the tree top point and the critical point. Then the average width is calculated for each tree from the four radii examined.

[37] The output is a simple text file indicating the number of trees identified along with their coordinates, heights, and crown radii.

### 3.5. Detection Accuracy

[38] Detection accuracy is assessed by comparing prior knowledge of tree characteristics with the estimated tree characteristics from the two tree detection and delineation algorithms. This accuracy method is defined by *Pouliot et al.* [2002]. Overall accuracy of the detection and delineation methods can be defined as

$$AI(\%) = \left[\frac{(n-(O+C))}{n}\right] \times 100 \qquad (5)$$

[39] $AI$ is an accuracy index in percent, $O$ and $C$ represent the number of omission and commission errors, and $n$ is the total number of trees in the image to be detected. The purpose of the index is to count all error against the correct number of trees to be detected. Commission errors are where local maxima are not the crown tops, and Omission errors are where crown maxima were not detected.

[40] To evaluate the individual crown width and height measurement error, the root mean square error (RMSE) of the derived values as a percentage of the mean true values was calculated as:

$$\mathrm{RMSE}(\%) = 100 \times \left[\sqrt{\frac{\left(\Sigma(I_i - G_i)^2\right)}{n}}\right] / G \qquad (6)$$

where $G_i$ is the ground measurement value, $G$ is the mean value of ground measurement values, $I_i$ is the derived tree value, and $n$ is the number of observations.

## 4. Results and Discussion

### 4.1. Elevation Models

[41] DTMs were created for the meander sections considered in the Garonne and Allier rivers using a point cloud data set comprising of first and last pulse data with a cell size of 10 m, as described in section 3.1. First and last pulse data were used instead of just last pulse information. This is due to the fact that some of the ground hits returned higher elevation values for the last pulse than the first pulse, attributed to noise from the airborne receiver. This noise was centimetric or decimetric at most on the ground and was also randomly distributed with space, so any accuracy measures would have be difficult to implement. Including more points in a standard sized grid cell does not affect its indication of the minimum elevation coordinate. A 10 m grid cell size was used to account for the size of dense tree canopies, as potentially no last pulse data is retrieved if considering smaller windows. The 10 m resolution for the terrain model was chosen as the optimum resolution where the terrain was effectively represented even in dense canopies. Smaller grid cell sizes would have caused the terrain to be significantly higher in mature forests, and would have resulted in false individual tree height results. An example of the terrain model for the Verdun meander is shown below in Figure 3, where the main differences between the two models can be noted around the river channel and on the immediate floodplain.

### 4.2. Detectable Tree Variable Regressions

[42] The regression equations for both the TDCS and TreeVaW methods are presented in Table 2. The regressions between crown width and tree height produce high coefficients of determination ($R^2$) values of around 0.9 for the

**Table 2.** Total Tree Height and Crown Width Regressions Calculated From Ground Measurements of Poplars in the Three Sites of Verdun, Monbequi, and Châtel-de-Neuvre

| Meander Site | Allometric Power Law Regression | $R^2$ | Linear Regression | $R^2$ |
|---|---|---|---|---|
| Verdun planted poplar | $CW = 0.872H^{0.696}$ | 0.914 | $CW = 0.256H + 1.780$ | 0.896 |
| Monbequi natural poplar | $CW = 1.146H^{0.616}$ | 0.551 | $CW = 0.272H + 1.875$ | 0.454 |
| Allier natural poplar | $CW = 0.358H^{1.033}$ | 0.912 | $CW = 0.403H - 0.319$ | 0.867 |

Verdun and Châtel-de-Neuvre sites for both linear and power relationships. For the Monbequi site, around 45–55% of the variability in a data set is accounted for by the statistical model. This may result in the detection and measurement of trees to be of lower accuracy at the Monbequi site than the other sites, for both methods.

[43] For the natural trees measured in the Châtel meander, crown width and tree height increase at almost the same rate (isometric allometry), while the tree measured at in the Garonne River floodplain had a negative allometry. The Monbequi and Verdun regressions suggest that the trees grow vertically at a faster rate than the increase in crown width. If the trees are densely spaced as at the Monbequi site, then trees must produce grow upward quickly to accommodate the extra demand for light, while for the Châtel meander, the forest compete less for space.

### 4.3. Tree Identification Accuracy

[44] There is a need to ascertain the accuracy of the methods deployed in this study as well as calculating the stem diameters at each site. The outputs of the methods are also compared to the ground-derived measurements. First, Table 3 presents identification and delineation accuracies. The sites described in Table 3 are the three planted poplar sites at Verdun (young (VY), intermediate (VI), and mature (VM) tree ages) and natural poplar riparian forest at Monbequi (Mnb).

[45] Both methods showed average tree identification accuracies of over 80% meaning that over 270 trees were accurately identified of the 331 measured. Both methods identified planted hybrid poplars (Verdun site) better than natural riparian poplar (Monbequi site). The TreeVaW method identified greater than 95% of the trees in the planted poplar site, while only ~70% in the natural forest. The TDCS method identified slightly fewer of the planted trees (greater than 90%), yet the trees identified in the natural forest were as high as 82%. The commission errors for the first method steadily increased as the forested section became denser from errors of only 1.75% in the young planted poplar site to over 20% in the natural dense forest of Monbequi. The TreeVaW method generally produces larger random commission errors, with the largest (~35%) being again for the natural forested section. The accuracy indices (equation (1)) take into account the trees omitted and those that did not represent a measured tree. Using both methods, the numbers of crowns detected were fewer than the numbers of trees identified on the ground. Accuracy indices of crown widths were over 20% higher for the TDCS method than for the TreeVaW method. Spacing accuracies were within one pixel for the planted site, and the accuracy of the actual single trunk locations was centimetric. The spacing accuracies of both methods were very similar. For the Monbequi site, distances from measured tree locations were about 2 m. The large error here may be accounted for first by the method of identifying the UTM coordinates of the tree locations, which was achieved by fixing transects of know UTM coordinates in the site, and measuring perpendicular distances from the transect line. Second, for multiple trees, a middle point between the trunks was taken as the tree center.

[46] An increase in omission errors may have the overall effect of decreasing actual spacing for specific sites. An increase in commission errors may have the opposite effect of increasing the actual spacing of the sites, but may also decrease or increase the actual tree maxima or crown width values for the trees. The number of surplus trees falsely identified may therefore cause further error in estimating the stem resistance of a vegetated patch. Therefore, it may be

**Table 3.** Tree and Crown Identification Accuracies for the Four Sites Investigated on the Garonne River[a]

| Sites | Number of Trees Measured | Trees Accurately Identified, % | Commission Errors for Identified Trees, % | Accuracy Index for Identified Trees | Accuracy Index for Identified Crowns | Spacing Accuracy (Average Distance), m |
|---|---|---|---|---|---|---|
| | | | *Method 1 (TDCS)* | | | |
| VY | 56 | 100.00 | 1.75 | 98.21 | 98.21 | 0.429 |
| VI | 30 | 93.33 | 7.14 | 86.67 | 86.67 | - |
| VM | 110 | 91.18 | 17.82 | 80.00 | 78.18 | 0.569 |
| Mnb | 95 | 82.10 | 20.51 | 65.26 | 61.05 | 2.096 |
| Total | 311 | 84.57 | 12.22 | 88.42 | 86.50 | |
| | | | *Method 2 (TreeVaW)* | | | |
| VY | 56 | 100 | 5.35 | 94.64 | 67.85 | 0.426 |
| VI | 30 | 96.67 | 27.58 | 70.00 | 53.33 | - |
| VM | 110 | 97.27 | 5.61 | 85.45 | 91.81 | 0.575 |
| Mnb | 95 | 69.47 | 34.84 | 45.26 | 42.11 | 2.220 |
| Total | 311 | 82.96 | 12.86 | 67.84 | 62.7 | |

[a]The accuracies are shown for the two identification and delineation methods (TDCS/TreeVaW). The Allier results are not presented here, as no commission information was possible.

**Table 4.** Transfer Functions to Interpolate the Below-Canopy Stem Diameters From the Known Above-Canopy Characteristics of Tree Height and Crown Diameter[a]

| Sites | Height and Trunk Diameter | $R^2$ | Crown Width and Trunk Diameter | $R^2$ |
|---|---|---|---|---|
| VY | $H = 116.98D^{1.154}$ | 0.38 | $CW = 94.19D^{1.465}$ | 0.50 |
| VI | $H = 106.17D^{1.206}$ | 0.80 | $CW = 45.94D^{1.314}$ | 0.54 |
| VM | $H = 68.88D^{0.951}$ | 0.66 | $CW = 21.18D^{0.895}$ | 0.57 |
| Mnb | $H = 33.85D^{0.705}$ | 0.64 | $CW = 10.23D^{0.435}$ | 0.79 |
| Châtel | $H = 35.12D^{0.685}$ | 0.80 | $CW = 13.66D^{0.708}$ | 0.68 |

[a]D, canopy stem diameters; H, tree height; and CW, crown diameter.

expected that TDCS method rather than TreeVaW method will produce more accurate roughness values compared to the measured trunk diameters and spacing.

[47] The results of the identification compared positively to other research to have attempted automatic tree identification. *Pouliot et al.* [2002] measured accuracy indices for the detection of black spruce and jack pine crop trees of a maximum of 91%. *Tiede et al.* [2005] measured detection accuracies of 51% for a mixed natural boreal forest in eastern Germany, and *Maltamo et al.* [2004] detected around 40% of trees in a mixed natural boreal forest reserve. *Roberts et al.* [2005] correctly identified loblolly pine trees in Texas with a detection average of 83% with a range from 68% to 93%, and identification accuracy indices averaged to about 89% with omission errors rising to 33%.

### 4.4. Transfer Functions

[48] Transfer functions in the form of allometric power laws were determined from field measurements. The purpose of these is to determine the below-canopy stem diameters from detectable canopy parameters such as crown width and overall tree height. These transfer functions are described below in Table 4. The relationships in Table 4 are all in units of meters, and the diameter is the total diameter of the stems associated with an individual tree crown, be it single or multiple. Plots of the transfer functions and of their natural variability are shown in Figure 4.

[49] The allometric regressions produced had low to medium coefficients of determination ($R^2$) of 0.38 for the height-diameter regression of the young planted poplars, to 0.80 for the height-diameter regressions of the mature planted poplars and the natural poplars in Châtel-de-Neuvre. The differences in these $R^2$ values arise in part from the small sample sizes for some areas, and also from the lack of variation in age in others. The crown width regression that best fits the raw point values is the natural poplar forest of Monbequi with an $R^2$ value of 0.79.

[50] The slopes of the curves, or the scaling exponents, are also important indicators in comparing regressions between the sites. For the planted polar, the height-total diameter regressions produce lower scaling exponents with increase in age from $\alpha = 1.154$ for young poplars to $\alpha = 0.951$ for mature poplars. Therefore as the planted tree grows, it gains height at a faster rate than its increase in the trunk diameter. Subsequently, to support the weight of the taller tree, the trunk starts increases in width. The same would apply to the crown width for the three planted poplar age groups.

[51] In the natural riparian forests of Monbequi and Châtel-de-Neuvre, the trunk numbers on average are greater than for the planted trees at the Verdun sites. Crown widths grow larger in the Châtel-de-Neuvre site ($\alpha = 0.708$) as it is populated by sparser poplar forest than Monbequi ($\alpha = 0.435$), while tree heights grow by almost the same amount in both regions.

[52] The scaling exponents for the height-trunk diameter and crown width-trunk diameter relationships of all planted poplars are $\alpha = 0.879$ and $\alpha = 0.612$, respectively. These come closer to the natural poplar forest scaling exponents of around $\alpha = 0.7$ for the height-trunk diameter regression and $\alpha = 0.43–0.7$ for the crown width-trunk diameter regression. These values are also quite close to the allometric scaling exponents in the literature. *Niklas* [1994] described a scaling exponent for tree height-trunk diameter of a large number of gymnosperms and angiosperms to be around $\alpha = 0.73$, and the crown width-trunk diameter exponent for angiosperms to be around $\alpha = 0.6–0.79$. *King* [1991] evaluated a scaling exponent between tree height and trunk diameter for gymnosperms and angiosperms to be between 0.71 and 0.101, and *McMahon* [1973] described a theoretical allometric power law for all vegetation in the form $H = D^{0.5}$.

### 4.5. Tree Height Estimate

[53] Tree heights and crown widths of all the areas studied were compared against the ground-measured values, the root-mean-square error (RMSE) being used as an indicator of deviation of the estimated values from the measured values. The RMSE is a measure of the difference between values determined by any method and values measured in the field. The RMSE equation is defined in equation (2). Table 5 presents the RMSE values for the derived heights and crown widths of the two tree detection and crown delineation methods deployed in this study. The diameters derived from the transfer functions in Table 4 are also presented for each study area in Table 5.

[54] The RMSE assesses deviation from the measured values for a certain sample size, and therefore takes into account the omission of identified trees. The largest deviations from the measured values for tree heights are around 26%, while the smallest deviations are around 12% of the measured values. The deviations for the two methods are almost the same, with the TreeVaW method having an average RMSE value for tree heights less than 1% greater than the TDCS method. The main difference between the two methods is the large RMSE value for mature natural poplars at the Châtel-de-Neuvre site, where the TreeVaW method reports tree height errors of 26.73% compared to the TDCS method value of 13.90%. This discrepancy may be due to false identifications of measured trees, or the true identifications with random errors in tree heights.

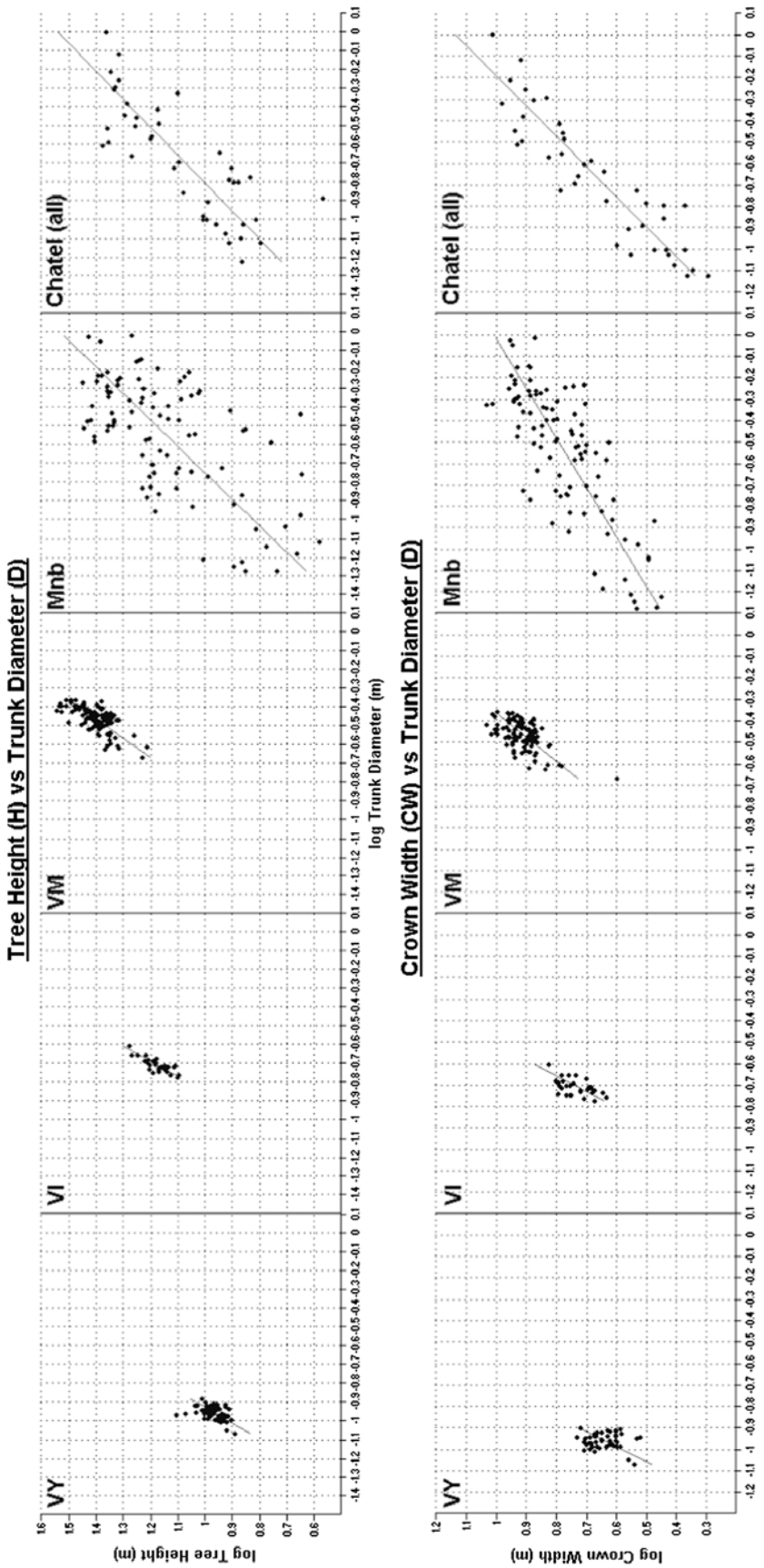


**Figure 4.** Transfer plots for both tree heights and crown widths versus trunk diameters for all the specific sites in this study. The two sites on the Châtel meander are aggregated for a stronger regression.

**Table 5.** RMSE for the Calculated Tree Heights and Crown Widths Identified for Each of the Six Areas[a]

| Sites | RMSE for Tree Heights, % | RMSE for Crown Widths, % | RMSE of Diameter Derived From Heights, % | RMSE of Diameter Derived From Crown Widths, % |
|---|---|---|---|---|
| | | *Method 1 (TDCS)* | | |
| VY | 25.61 | 53.76 | 22.55 | 35.29 |
| VI | 16.10 | 57.43 | 13.39 | 47.78 |
| VM | 11.96 | 70.01 | 13.92 | 74.36 |
| Mnb | 26.60 | 55.84 | 56.87 | 89.88 |
| ChY | 10.65 | 72.65 | 47.98 | 92.37 |
| ChM | 13.90 | 49.03 | 44.21 | 75.25 |
| Total | 18.88 | 61.77 | 31.55 | 70.94 |
| | | *Method 1 (TreeVaW)* | | |
| VY | 25.56 | 61.78 | 22.53 | 23.82 |
| VI | 16.41 | 52.79 | 13.45 | 44.77 |
| VM | 12.05 | 39.43 | 13.96 | 42.18 |
| Mnb | 22.75 | 37.19 | 55.05 | 70.24 |
| ChY | 17.85 | 40.00 | 46.80 | 70.76 |
| ChM | 26.73 | 48.44 | 45.17 | 59.75 |
| Total | 19.04 | 44.35 | 31.03 | 50.15 |

[a]The RMSE of the derived diameters from the transfer function described in Table 4 are also presented. The sites are defined as the meander and the forest type. These are Verdun young planted (VY); Verdun intermediate age planted (VI); Verdun mature planted (VM); Monbequi matural (Mnb); Châtel young natural (ChY); and Châtel mature natural (ChM).

[55] In both methods, the height deviations became less with the larger more mature planted poplars from around 26% RMSE to 12% RMSE at the Verdun site. This may be explained by the fact that larger trees have a larger crown, and therefore a broader surface to detect a treetop or near-treetop hit. In general, the RMSE values for the planted and natural poplar forests were not very different and ranged from deviations of around 14% to 26% for both detection methods.

[56] All tree height values for both methods were underestimated, by 6% for the TDCS method, and 7% for the TreeVaW method. Underestimation of tree heights is a commonly observed attribute of airborne lidar methods. This underestimation has been credited to lidar points hitting tree crowns and missing the apices due to the size of the footprint [*Roberts et al.*, 2005]. *Maltamo et al.* [2004] also investigated underestimates of airborne lidar total tree heights in forest sections of Norway spruce and Scots pine and suggested using a tree height correction linear regression formula. *Roberts et al.* [2005] produced an average error of remotely sensed tree heights while investigating loblolly pine plantations ranging from −3.6 m to 2.5 m. This was achieved by flying the instruments at 360 m and achieving a horizontal point precision of 0.4 m. In this study, the point cloud data was between 1.5 and 2.5 m on average. The average bias in heights for all sites was around 1.59 ± 2.87 m for the TDCS method and 1.70 ± 2.77 m for the TreeVaW method. Biases are not expected to be consistent as the forests in this study are of varying shapes, ages, and densities.

### 4.6. Crown Width Estimate

[57] The root-mean-square error (RMSE) values for crown widths are shown in Table 5. The largest deviations from the measured values for crown widths are around 72%, while the smallest deviations are around 37% of the measured values. These deviations are much larger than those for the tree heights. The TDCS method delineated crowns with average errors of greater than 60%, while the TreeVaW method delineated crowns to a better extend with an average error of around 45%. The RMSE values between the planted and natural poplar forests did not show any clear differences between methods. The crown widths based on the TDCS method seem to deviate more than those based on the TreeVaW method, yet both errors are two to three times the height errors.

[58] In fact, the crown widths derived from the TDCS method underestimated the measured values by 59.6%, with a bias of 2.76 ± 3.14 m. The TreeVaW method also underestimated the crown widths by around two thirds (69.6%), with a bias of 1.094 ± 3.05 m. Crown diameter is quite difficult to estimate, whether remotely or from the ground. Estimating crown diameters remotely assumes that crowns are circular, while in fact they tend to be asymmetrical with irregular edges, even when crowns are completely detached from one another. Also the edges of crowns are extremely difficult to determine in dense forested sections, due to the overlapping of individual crowns. In smaller crowns, edges may be missed completely, returning ground hits to the airborne sensor. Measurement of crown diameters in the field is equally difficult. Field measurements were produced where the edge of the crown was defined as the edge of pronounced branches in four directions. The branches could be up to 20 m above the standing position, so large errors ensue. Also the four geometric directions of measurement may not have been perpendicular, and crown radii may have followed the direction of a large branch.

### 4.7. Trunk Diameter Estimation

[59] Diameters were derived for each site, using the relevant transfer functions in Table 4. Table 5 shows the RMSE values for the derived trunk diameter values against the stem diameters measured in the field. On average, the trunk diameters derived from the calculated heights for both the TDCS and TreeVaW methods of tree detection deviated by about 30% from the measured values. The diameters

derived from crown widths calculated from the TDCS method produced RMSE values of up to 92% with an average percentage from all sites of 71%. Generally, the planted poplars produced the best estimates of total trunk diameters.

[60] On the whole, the trunk diameters estimated from the transfer functions always underestimated the ground-measured values. The TDCS method underestimated the total trunk diameters by 14% for total height-derived calculations, and 60% for crown width-derived calculations. The TreeVaW method underestimated the total trunk diameters by 22% and 46% for total height and crown width-derived measurements, respectively. Diameters measured in the field had a fairly high accuracy due to the method of measurement and estimation. All stem circumferences were measured at breast height (1.4 m) with centimetric precision, using a 1 m tape; however, there are errors in estimating diameters because of the assumption of a circular cross section. Nevertheless, the deviations of the derived diameters from those measured can be largely attributed to inaccuracies in estimating tree heights and crown diameters from the lidar data.

### 4.8. Resistance Estimates

[61] Stem roughness was calculated using equation (3) and converting the Darcy-Weisbach $f$ to Manning's $n$ using equation (4), for comparison to the tabled roughness values of *Chow* [1959] and the *Arcement and Schneider* [1989]. Average total trunk diameters were used for each of the six study areas, and the drag coefficient of each site was calculated using equation (2). Results are presented in Figure 5. The stem roughness calculations for all four of the Garonne sites are compared to the Manning's $n$ values derived from the measured variables in the field, acting as a control. No trunk spacing estimates were obtained for the two sites on the Allier River, so no control is available for these. Roughness coefficients ($C_d$) calculated from equation (2) were very close to the advised value of 1.0–1.5 when considering trunks roughness. The $C_d$ values calculated for the TDCS method ranged from 0.96–1.25, and for the TreeVaW method ranged from 0.94 to 1.23.

[62] For three out of the four Garonne sites (Figures 5a, 5c, and 5d), the roughness values derived from the TDCS method total tree height estimations were the closest to the ground-measured plots. The young planted poplar, mature planted poplar, and the natural poplar forest sites show a difference between the two sets of 2.3%, 7.6%, and 41%, respectively. For the intermediate-aged poplar, the heights determined from the TreeVaW method produce the closest roughness values to the ground-based estimates, with a difference between them of 23%. For the roughness plots described, the tree height estimations in both methods produced the closest roughness values to the ground control, with an average difference between the two of just over 14%. The plot that fitted the ground-derived roughness values worst was the crown-width-derived roughness values using the TDCS method for most occasions, with average differences from the ground-measured Manning's $n$ values of 45%.

[63] An indicator of how well the two methods aid in defining the stem roughness of each of the six study areas is their percentage difference. There may be a bias here in that the sample of trees in each area is not the same, and that the allometric equations described in Table 4 do not have the same regression fits. The total variation (TV) for the roughness plots of each area is stated in Figures 5a–5f. Variations in plots for the planted poplars at Verdun increase from 11.4% to 40.4% with an increase in tree age. Variations in roughness in the natural forests at Monbequi and Châtel-de-Neuvre are steady at about 48 – 57%. Therefore forests with denser vegetation produce roughness estimates that are more variable than sparser forests, and also planted and ordered forests produce less variable roughness estimates than natural forests of varied ages.

[64] If the flow depth value of 1.4 m is taken (as diameter at breast height), the range in Manning's $n$ values of the four plots for each study area are, $n$ = 0.025–0.028 for the young planted poplars at Verdun, $n$ = 0.026–0.041 for the intermediate aged planted poplar at Verdun, $n$ = 0.028–0.046 for the mature planted poplar at Verdun, $n$ = 0.040–0.078 for the Monbequi site, $n$ = 0.025–0.058 for the young poplar forest at Châtel-de-Neuvre, and $n$ = 0.028–0.063 for the mature poplar forest at Châtel-de-Neuvre. It is expected that forests with larger trunks will result in higher roughness coefficients due to the increase frontal area in contact with the floodwater. From the values just stated, this increase in roughness can be seen from the Châtel-de-Neuvre sites as well as the Verdun planted forest sites of different ages. Mature natural forests would also tend to offer a more variable spacing of trunks, and a higher density of trunks per individual tree identified, increasing the Manning's $n$ estimates. The highest roughness values are those from the dense natural forest at Monbequi. In this site, the density of trunks is the highest, and the number of trunks per individual tree crown is the highest. Therefore combining the total diameter and decreased spacing produce a much higher roughness estimate than the other sites.

[65] The estimates stated above can be compared to the standard roughness coefficients stated by *Chow* [1959] and also by the roughness coefficient guidelines set out by *Arcement and Schneider* [1989] briefly stated in Table 6. Roughness coefficients for the three natural sites are close to the range of values stated for flow below branches, although toward the lower end of the spectrum ($n$ = 0.25 – 0.078). This can be expected as roughness coefficients for all the sites underestimated the ground-measured results. The planted poplar roughness values at Verdun can also be related to the simple trunk roughness coefficients of $n$ = 0.03–0.05 from *Chow* [1959] in Table 6.

## 5. Conclusions

[66] The TDCS (tree detection and crown segmentation) method produced slightly better results than the TreeVaW method developed by *Kini and Popescu* [2004] as far as individual tree detection and tree height accuracies are concerned, but worse in terms of crown diameters. The TDCS accurately determined 85% of the trees investigated with 12% commission errors, and the TreeVaW method accurately identified 83% of the trees with 13% commission errors. The accuracy index of tree heights estimated using the first method was 88% compared to 68% for the second method. The TreeVaW method seemed largely to overestimate the number of trees both in planted poplar riparian

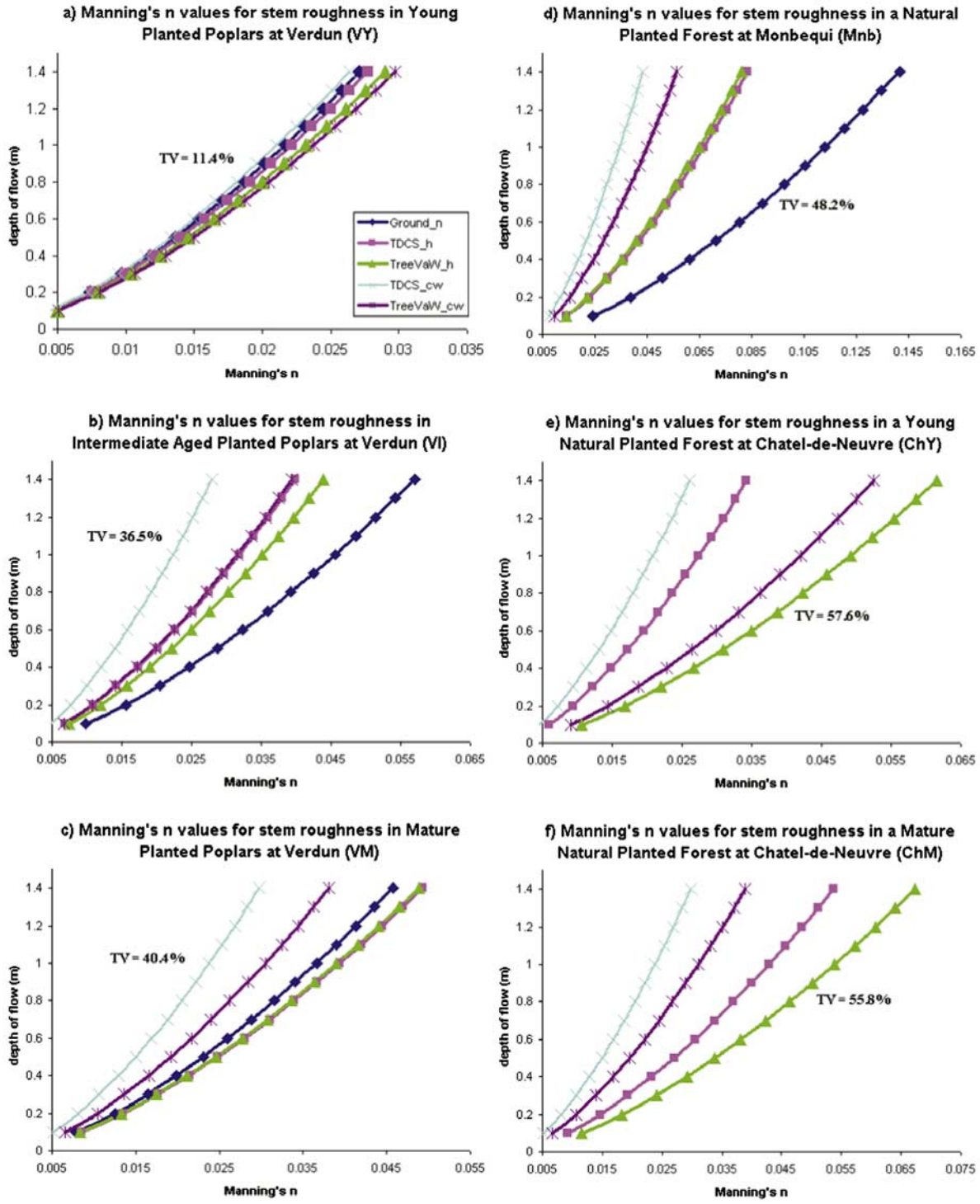


**Figure 5.** Manning's *n* values for the six sites studies with flow depth until diameter at breast height (1.4 m). The five plots are the ground measurement-derived roughness (Ground_n), the total height/crown width estimated trunk diameters for deriving roughness from the TDCS method (TDCS_h; TDCS_cw), and the total height/crown width estimated trunk diameters for deriving roughness from the TreeVaW method (TreeVaW_h; TreeVaW_cw). The total variations (TV) between these four plots are also stated as a percentage.

forests and in natural riparian forests, yet the crown width root mean square errors (RMSE) indicated more accurate results than those of the TDCS determined crown widths. Because of the large commission errors of the TreeVaW method, though, trunk spacing was denser than that measured in the field, and this would have influenced roughness estimates based on the Darcy-Weisbach friction factor in equation (3). Transfer functions (allometric power laws)

**Table 6.** Values of Manning's *n*

| Area Description | Minimum | Normal | Maximum |
|---|---|---|---|
| Cleared land with stumps[a] | 0.030 | 0.040 | 0.050 |
| Stumps w/undergrowth[a] | 0.050 | 0.060 | 0.080 |
| Flooding below branches[a] | 0.080 | 0.100 | 0.120 |
| Natural Forest flooding below canopy[b] | 0.065 | 0.09 | 0.140 |

[a]From *Chow* [1959].
[b]From *Arcement and Schneider* [1989].

derived from ground measurements proved to be valuable both in the crown delineation processes, and in estimating the underlying trunk areas. Resulting stem roughness values for both planted poplars and natural poplars fell within the range of Manning coefficients described by *Chow* [1959] and the *Arcement and Schneider* [1989]. Planted poplar forests at Verdun produced roughness coefficients ranging from $n = 0.033-0.062$ and natural forests at Monbequi and Châtel-de-Neuvre resulted in roughness values of around $n = 0.04 - 0.1$.

[67] Thus, the limiting factor in this study was the ability to measure crown width accurately, both from the delineation algorithms, and from the ground. Yet, for the purpose of estimating stem frontal areas, using tree heights resulted in 2.5–10% underestimates of stem roughness values in planted poplar, and 40% underestimation for the dense natural forest at Monbequi (using the ground-measured derived roughness coefficients as the control). Most detection and delineation work has been done on crop trees with an even spacing, or in natural forests of large pine, but little work has been done which has included very dense natural riparian forests. This method has provided a way to extract roughness parameters for forest stems in complex riparian environments.

[68] Current airborne remote sensing methods can measured tree heights much more accurately than crown widths, especially when dealing with dense forests where crowns are interwoven. Therefore for the parameterization of flow resistance, the transfer functions or relationships between tree height and trunk diameter are very significant, and these relationships are a necessary tool to estimate the projected area of simple below-canopy characteristics. Hence, this work introduces the need to further establish functional relationships for a variety of riparian vegetation species and types including bushes, and particularly in areas that are dominated by dense floodplain forests and shrubs. A subsequent development would be to consider the vertical distribution of the projected area, especially in the canopy layers. If flow enters the canopy levels of woody vegetation, then new roughness values need to be estimated with more complex considerations of crown frontal area, incorporating leaf-on and leaf-off conditions. New remote sensing techniques would need to be implemented for a more complex consideration of the canopy architecture. Terrestrial laser scanning with millimeter point resolution and a 140-degree vertical, 360-degree horizontal swath width can be used to conceptualize individual trees into the third dimension.

[69] Any research on vegetation characteristics and resistance parameterization is rare. Hydraulic modeling has been hindered because of the lack of this type of data for model calibration and validation. Thus better parameterization of simple trunk and more complex canopy roughness for various vegetation types is a necessity. Also, the gathering of stage and discharge data would be immensely valuable for the tested field site to be able to test the actual sensitivity of the parameters obtained, and against other estimates of vegetation resistance.

[70] **Acknowledgments.** This paper is the result of airborne lidar data obtained from a NERC project in June 2006. This research was supported by the British Society for Geomorphology (BSG) and from the William Vaughan Lewis and Phillip Lake Funds.

## References

Adams, J. C., and J. H. Chandler (2002), Evaluation of lidar and medium scale photogrammetry for detecting soft-cliff coastal change, *Photogramm. Rec.*, *17*(99), 405–418, doi:10.1111/0031-868X.00195.

Andersen, H. E., S. E. Reutebuch, and G. F. Schreuder (2001) Automated individual tree measurement through morphological analysis of a lidar-based canopy surface model, paper presented at of the First International Precision Forestry Cooperative Symposium, Inst. of For. Resour., Univ. of Wash., Seattle, 17–20 June.

Anderson, E. S., J. A. Thompson, D. A. Crouse, and R. E. Austin (2006), Horizontal resolution of data density effects on remotely sensed lidar-based DEM, *Geoderma*, *132*, 406–415, doi:10.1016/j.geoderma.2005.06.004.

Arcement, G. J., Jr., and V. R. Schneider (1989), Guide for selecting Manning's roughness coefficients for natural channels and flood plains, U.S. Geol. Surv. Water Supply Pap., 2339.

Brandtberg, T., T. A. Warner, R. E. Landenberger, and J. B. McGraw (2003), Detection and analysis of individual leaf-off tree crowns in small footprint, high sampling density lidar data from the eastern deciduous forest in North America, *Remote Sens. Environ.*, *85*, 290–303, doi:10.1016/S0034-4257 (03)00008-7.

Chow, V. Y. (1959), *Open Channel Hydraulics*, McGraw-Hill, New York.

Cobby, D. M., D. C. Mason, M. S. Horritt, and P. D. Bates (2003), Two-dimensional hydraulic flood modelling using a finite-element mesh decomposed according to vegetation and topographic features derived from airborne scanning laser altimetry, *Hydrol. Process.*, *17*, 1979–2000, doi:10.1002/hyp.1201.

Culvenor, D. S. (2002), TIDA: An algorithm for the delineation of tree crowns in high spatial resolution remotely sensed imagery, *Comput. Geosci.*, *28*, 33–44, doi:10.1016/S0098-3004(00)00110-2.

Décamps, H., M. Fortune, F. Gazelle, and G. Pautou (1988), Historical influence of man on the riparian dynamics of a fluvial landscape, *Landscape Ecol.*, *1*(3), 163–173, doi:10.1007/BF00162742.

de Jong, J. (2005), Modelling the influence of vegetation on the morphodynamics of the river Allier, M.Sc. thesis, Delft Univ., Delft, Netherlands.

Fathi-Maghadam, M., and N. Kouwen (1997), Nonrigid, nonsubmerged, vegetative roughness on floodplains, *J. Hydraul. Eng.*, *123*(1), 51–57, doi:10.1061/(ASCE)0733-9429(1997)123:1(51).

Hyyppä, J., O. Kelle, M. Lehikninen, and M. Inkinen (2001), A segmentation-based method to retrieve stem volume estimates from 3-D tree height models produced by laser scanners, *IEEE Trans. Geosci. Remote Sens.*, *39*, 969–975, doi:10.1109/36.921414.

Järvelä, J. (2002), Flow resistance of flexible and stiff vegetation: A flume study with natural plants, *J. Hydrol.*, *269*(1–2), 44–54, doi:10.1016/S0022-1694(02)00193-2.

Järvelä, J. (2004), Determination of flow resistance caused by non-submerged woody vegetation, *Int. J. River Basin Manage.*, *2*(1), 61–70.

Kanopoulos, N., N. Vasanthavada, and R. L. Baker (1988), Design of an image edge-detection filter using the Sobel operator, *IEEE J. Solid State Circuits*, *23*(2), 358–367, doi:10.1109/4.996.

King, D. A. (1991), Tree allometry, leaf size and adult tree size in old growth forests of western Oregon, *Tree Physiol.*, *9*, 369–381.

Kini, A., and S. C. Popescu (2004), TreeVaW: A versatile tool for analyzing forest canopy lidar data: A preview with an eye towards future, paper presented at ASPRS 2004 Fall Conference, Am. Soc. of Photogramm. and Remote Sens., Kansas City, Mo., 12–16 Sept.

Koukoulas, S., and G. A. Blackburn (2005), Mapping individual tree location, height and species in broadleaved deciduous forest using airborne lidar and multi-spectral remotely sensed data, *Int. J. Remote Sens.*, *26*(3), 431–455, doi:10.1080/0143116042000298289.

Kouwen, N., and M. Fathi-Maghadam (2000), Friction factors for coniferous trees along rivers, *J. Hydraul. Eng.*, *126*(10), 732–740, doi:10.1061/(ASCE)0733-9429(2000)126:10 (732).

Kouwen, N., T. E. Unny, and A. M. Hill (1969), Flow retardance in vegetated channels, *J. Irrig. Drain. Div.*, *95*(2), 329–342.

Lane, S. N., T. D. James, H. Pritchard, and M. Saunders (2003), Photogrammetric and laser altimetric reconstruction of water levels for extreme

flood event analysis, *Photogramm. Rec.*, *18*(104), 293–307, doi:10.1046/j.0031-868X.2003.00022.x.

Lindner, K. (1982), Der Strömungswiderstand von Pflanzenbeständen, Doctoral thesis, Mitt. 75, Leichtweiss-Inst. für Wasserbau, Tech. Univ. Braunschweig, Brunswick, Germany.

Lloyd, C. D., and P. M. Atkinson (2002), Deriving DSMs from lidar data with kriging, *Int. J. Remote Sens.*, *23*(12), 2519–2524, doi:10.1080/01431160110097998.

Lohr, U. (1998), Digital elevation models by laser scanning, *Photogramm. Rec.*, *16*(91), 105–109, doi:10.1111/0031-868X.00117.

Maltamo, M., K. Mustonen, J. Hyyppä, J. Pitkänen, and X. Yu (2004), The accuracy of estimating individual tree variables with airborne laser scanning in boreal nature reserve, *Can. J. For. Res.*, *34*, 1791–1801, doi:10.1139/x04-055.

Maltamo, M., K. Eerikainen, P. Packalen, and J. Hyyppä (2006), Estimation of stem volume using laser scanning-based canopy height metrics, *Forestry*, *79*(2), 217–229, doi:10.1093/forestry/cpl007.

Mason, D. C., D. M. Cobby, M. S. Horritt, and P. D. Bates (2003), Floodplain friction parameterisation in two-dimensional river flood models using vegetation heights derived from airborne scanning laser altimetry, *Hydrol. Process.*, *17*, 1711–1732, doi:10.1002/hyp.1270.

McCombs, J. W., S. D. Roberts, and D. L. Evans (2003), Influence of fusing lidar and multispectral imagery on remotely sensed estimates of stand density and mean tree height, *For. Sci.*, *49*, 457–466.

McMahon, T. A. (1973), Size and shape in biology, *Science*, *179*, 1201–1204, doi:10.1126/science.179.4079.1201.

Muller, E., H. Guilloy-Froget, N. Barsoum, and L. Brocheton (2002), Populus nigra L. en vallée de Garonne: Legs du passé et constraints du présents, *C. R. Biol.*, *325*, 1129–1141, doi:10.1016/S1631-0691(02)01519-6.

Niklas, K. J. (1994), *Plant Allometry: The Scaling of Form and Process*, 395 pp., Univ. of Chicago Press, Chicago, Ill.

Niklas, K. J. (2004), Plant allometry: Is there a grand unifying theory?, *Biol. Rev. Cambridge Philos. Soc.*, *79*, 871–889, doi:10.1017/S1464793104006499.

Pasche, E., and G. Rouvé (1985), Overbank flow with vegetatively roughened flood plains, *J. Hydraul. Eng.*, *111*(9), 1262–1278.

Peters, B., K. van Looy, and G. Kurstjens (2000), Pioniervegetaties langs grindrivieren: de Allier en de Grensmaas, *Nat. Maandblad*, *7*(89), 123–136.

Pitkänen, J., M. Maltamo, J. Hyyppä, and X. Yu (2003), Adaptive methods for individual tree detection on airborne laser based canopy height model, *Int. Arch. Photogramm. Remote Sens. Spatial Inf. Sci.*, *36*, 187–191.

Popescu, S. C., R. H. Wynne, and R. F. Nelson (2003), Measuring individual tree crown diameter with lidar and assessing its influence on estimating forest volume and biomass, *Can. J. Remote Sens.*, *29*(5), 564–577.

Pouliot, D. A., D. J. King, F. W. Bell, and D. G. Pitt (2002), Automated tree crown detection and delineation in high-resolution digital camera imagery of coniferous forest regeneration, *Remote Sens. Environ.*, *82*, 322–334, doi:10.1016/S0034-4257(02)00050-0.

Roberts, S. D., T. J. Dean, D. L. Evans, J. W. McCombs, R. L. Harrington, and P. A. Glass (2005), Estimating individual tree leaf area in loblolly pine plantations using lidar-derived measurements of height and crown dimensions, *For. Ecol. Manage.*, *213*, 54–70, doi:10.1016/j.foreco.2005.03.025.

Soille, P. (1999), *Morphological Image Analysis: Principles and Applications*, Springer, New York.

Stoesser, T., C. A. M. E. Wilson, P. D. Bates, and A. Dittrich (2003), Application of a 3D numerical model to a river with vegetated floodplains, *J. Hydroinf.*, *5*(2), 99–112.

Suárez, J. C., C. Ontiveros, S. Smith, and S. Snape (2005), Use of airborne lidar and aerial photography in the estimation of individual tree heights in forestry, *Comput. Geosci.*, *31*, 253–262, doi:10.1016/j.cageo.2004.09.015.

Tiede, D., G. Hochleitner, and T. Blaschke (2005) A full GIS-based workflow for tree identification and tree crown delineation using laser scanning, in *Proceedings of the ISPRS Workshop CMRT 2005 Object Extraction for 3D City Models, Road Databases and Traffic Monitoring—Concepts, Algorithms and Evaluation*, vol. XXXVI, Part 3/W24, edited by U. Stilla, F. Rottensteiner, and S. Hinz, pp. 9–14, Int. Soc. for Photogramm. and Remote Sens., London.

Yen, B. C. (2002), Open channel flow resistance, *J. Hydraul. Eng.*, *128*(1), 20–39, doi:10.1061/(ASCE)0733-9429(2002)128:1(20).

A. S. Antonarakis, M. Bithell, J. Brasington, and K. S. Richards, Department of Geography, Cambridge University, Downing Place, Cambridge, CB2 3EN, UK. (asa36@cam.ac.uk)

E. Muller, Laboratoire Dynamique de la Biodiversité, CNRS, 29, rue Jeanne Marvig, Haute-Garonne, F-31055 Toulouse Cedex 4, France.